Comparative Transcriptomic Analysis of A549 Cellular Responses to H1N1/WSN and H9N2 Influenza Infections

Lee Eugenie

18 April 2024

1. Background

Historically, efficient human-to-human transmission of strains like H1N1 has led to major influenza pandemics, notably in 1918 and 2009, highlighting the substantial public health risks posed by these viruses. The pandemic H1N1 influenza virus, which incorporated genetic material from avian, swine, and human influenza viruses, exemplifies the significant role of interspecies viral reassortment in the emergence of pandemic strains [1]. Avian Influenza A H9 subtype viruses discovered in wild avians and domestic poultry are classified as low pathogenic avian influenza (LPAI) viruses. The H9N2 virus has been found in bird populations across Asia, Europe, the Middle East, and Africa. There have been instances of H9N2 virus infections in humans, resulting primarily in mild upper respiratory symptoms [2].

Previous studies by Taye et al. explored the inter-species host gene expression differences elicited by human and avian influenza A virus strains [3, 4]. By using a system-based approach, this research enhances the understanding of the biological differences in how human and avian cells respond to H7N9 infection. It underscores the complexity of host-pathogen interactions and supports the development of more effective strategies to combat influenza outbreaks, particularly in zoonotic transmissions [3, 4]. This study extends these findings by comparing the differential activation of these pathways in A549 cells infected with H1N1/WSN and H9N2, providing a deeper understanding of strain-specific immune responses and identifying potential targets for therapeutic intervention. By extending this approach to include network analysis, this study identifies hub genes and integrates these findings with drug-target interaction data, potentially paving the way for novel antiviral drugs.

The field of transcriptome analysis has significantly evolved from its initial days of microarrays to the advanced era of next-generation sequencing (NGS) technologies. These advancements have enabled profiling of gene expression across various RNA species, revealing intricate molecular mechanisms underpinning human diseases and expanding the potential for these technologies in clinical diagnostics. [5] The transformation in transcriptome analysis has profoundly influenced drug discovery, particularly through profile-based inference methods that have moved from model organisms to more complex systems. [6]

This study employs a comprehensive bioinformatics approach to analyze transcriptomic data from A549 cells infected with H1N1/WSN and H9N2. The use of A549 cells offers a closer approximation of the human lung environment, which is crucial for in-depth studies of influenza A virus pathogenesis, host immune responses, and the screening of antiviral therapies [7]. By integrating pathway analysis, this research aims to delineate altered metabolic pathways and their roles in virus-host interactions, thus providing a deeper understanding of disease mechanisms. Through network analysis, the project seeks to identify key regulatory genes and pathways, spotlighting novel targets for therapeutic intervention and enhancing our preparedness for managing future influenza outbreaks.

2. Objective

This study aims to utilize a comprehensive bioinformatics approach to discern the unique and overlapping gene expression profiles in human A549 cells infected with avian influenza A virus H9N2 compared to those infected with the primarily human-infecting H1N1/WSN strain. By

conducting detailed pathway and network analyses, this research seeks to identify critical molecular targets and pathways that are influenced by both viral strains. These findings are expected to reveal potential points of therapeutic intervention and help in developing strategies that bridge species-specific viral responses to broader, more effective antiviral therapies. This comprehensive analysis enhances our understanding and preparedness for influenza outbreaks, potentially facilitating more effective management of the disease in human populations.

3. Materials and Methods

3.1. Data Retrieval and Preprocessing

The microarray dataset utilized in this study was sourced from the Gene Expression Omnibus (GEO) database under the accession number GSE31524 [3,4,8]. This dataset encompasses transcriptomic profiles obtained from A549 human cells infected with the A/WSN/33 (H1N1), and A/Duck/Malaysia/01 (H9N2) influenza virus. The dataset covers various time points post-infection (0, 2, 4, 6, 8, and 10 hours).

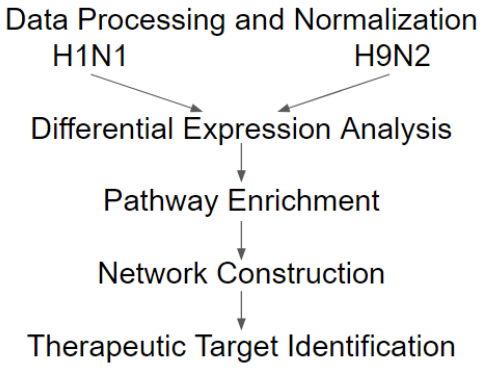

Figure 1. Overview of the workflow

Fig 1. illustrates the sequential workflow adopted for analyzing the gene expression data of A549 cells infected with H1N1/WSN and H9N2 strains. This workflow is designed to systematically process and analyze the data to identify potential therapeutic targets. Table 1 provides detailed experimental data for A549 cells infected with the Influenza A/WSN/33 (H1N1), and Influenza A/Duck/Malaysia/01 (H9N2) virus at various times post-infection. Each sample is identified by a GSM code, indicating its unique dataset within the GEO database. virus.

A

Sample	HPI[1]	MOI[2]	Replicate[3]
GSM781957	0	3	1
GSM781958	0	3	2
GSM781959	0	3	3
GSM781960	2	3	1
GSM781961	2	3	2
GSM781962	2	3	3
GSM781963	4	3	1
GSM781964	4	3	2
GSM781965	4	3	3
GSM781966	6	3	1
GSM781967	6	3	2
GSM781968	6	3	3
GSM781969	8	3	1
GSM781970	8	3	2
GSM781971	8	3	3
GSM781972	10	3	1
GSM781973	10	3	2
GSM781974	10	3	3

B

Sample	HPI[1]	MOI[2]	Replicate[3]
GSM781975	0	3	1
GSM781976	0	3	2
GSM781977	0	3	3
GSM781978	2	3	1
GSM781979	2	3	2
GSM781980	2	3	3
GSM781981	4	3	1
GSM781982	4	3	2
GSM781983	4	3	3
GSM781984	6	3	1
GSM781985	6	3	2
GSM781986	6	3	3
GSM781987	8	3	1
GSM781988	8	3	2
GSM781989	8	3	3
GSM781990	10	3	1
GSM781991	10	3	2
GSM781992	10	3	3

Table 1. Experimental data for A549 cells infected with Influenza A virus strains. **A**: Influenza A/WSN/33 (H1N1) infected A549 cells at 2, 4, 6, 8, 10 hours post infection. **B**: Influenza A/Duck/Malaysia/01 (H9N2) infected A549 cells at 2, 4, 6, 8, 10 hours post infection. [1]HPI (Hours Post Infection): The time after the virus has been introduced to the cell cultures. Time points listed are 0, 2, 4, 6, 8, and 10 hours. The "0" hour represents the control group prior to infection, serving as a baseline for comparative analysis. [2]MOI (Multiplicity of Infection): The number of virus particles added per cell during infection, set consistently at 3 for this experiment. [3]Replicate: The replication factor for the experiment at each time point, with three replicates per time point.

3.2. Microarray Data Normalization and Quality Control

The raw data were processed using the affy v.1.78.2 [9] in R v.4.3.1 (https://www.r-project.org/). Quality control checks were performed to ensure the integrity of the data, including assessments of background noise, labeling, and hybridization. The robust multi-array average (RMA) algorithm implemented within the affy was utilized for background correction, normalization, and summarization of the probe-level data.

3.3. Differential Expression Analysis

Differential expression analysis was performed using the limma v.3.56.2 [10]. The design matrix was constructed to model the time course of infection, with separate coefficients for each time point. Differentially expressed genes (DEGs) are identified by comparing gene expression at each time point (2, 4, 6, 8, and 10 hpi) to the baseline expression at 0 hpi. A linear model was fitted for each gene, and empirical Bayes moderation was applied to obtain stable estimates of gene expression changes over time. DEGs were identified using an adjusted p-value cutoff of less than 0.05 and an absolute log-fold change greater than 1.

3.4. Functional Enrichment Analysis

Gene Ontology (GO) [10,11] and Kyoto Encyclopedia of Genes and Genomes (KEGG) [12] pathway analyses were conducted on the set of DEGs using the clusterProfiler v.4.8.3 [13]. Enrichment analysis was performed to identify biological processes and pathways significantly over-represented among the upregulated and downregulated genes for both H1N1/WSN and H9N2 infected cells. Results were adjusted for multiple testing using the Benjamini-Hochberg method [14].

3.5. Network Visualization

Network visualization was conducted using Cytoscape software [15]. The STRING database has protein networks for more than 2000 organisms, including both physical interactions from

experimental data and functional associations from curated pathways, automatic text mining, and prediction methods [16]. It was used to query known and predicted protein-protein interactions. Hub genes are identified as genes that has many interactions with other genes, which play important roles in gene regulation and biological processes [17]. Hub genes were identified based on connectivity using the CytoHubba plugin [18] within Cytoscape, and subnetworks were explored for both H1N1/WSN and H9N2 virus infections.

3.6 Drug Prediction Using Hub Genes

A curated list of these 10 hub genes with highest degrees, identified from network visualization, was analyzed using the Enrichr platform (https://maayanlab.cloud/Enrichr/) [19] and uploaded the gene list for analysis. Libraries related to drug-target associations within the Drug Signatures Database (DSigDB) [20] was used to identify drugs and compounds showing potential interactions with the hub genes.

4. Results

4.1. DEG Identification

The study cataloged the gene expression changes in A549 cells following infection with H1N1/WSN and H9N2 strains, with a particular focus on the temporal progression of the host response. Table 2. illustrates the temporal dynamics of host cellular responses to H1N1/WSN and H9N2 infections, highlighting a more aggressive and extensive regulatory impact by H1N1/WSN in A549 cells, particularly in the later stages of infection.

Time Point	H1N1/WSN		H9N2	
(HPI)	Upregulated	Downregulated	Upregulated	Downregulated
2	0	0	4	0
4	4	3	0	0
6	30	10	81	13
8	1223	1365	185	39
10	2616	3924	315	117

Table 2. Number of DEGs in A549 cells over time. Differential expression analysis was performed by comparing the gene expression profiles of A549 cells at various post-infection time points (2, 4, 6, 8, and 10 hours post-infection, hpi) against their levels at 0 hpi. Genes were classified as differentially expressed based on an absolute log fold change greater than 1 and a p-value cutoff of 0.05.

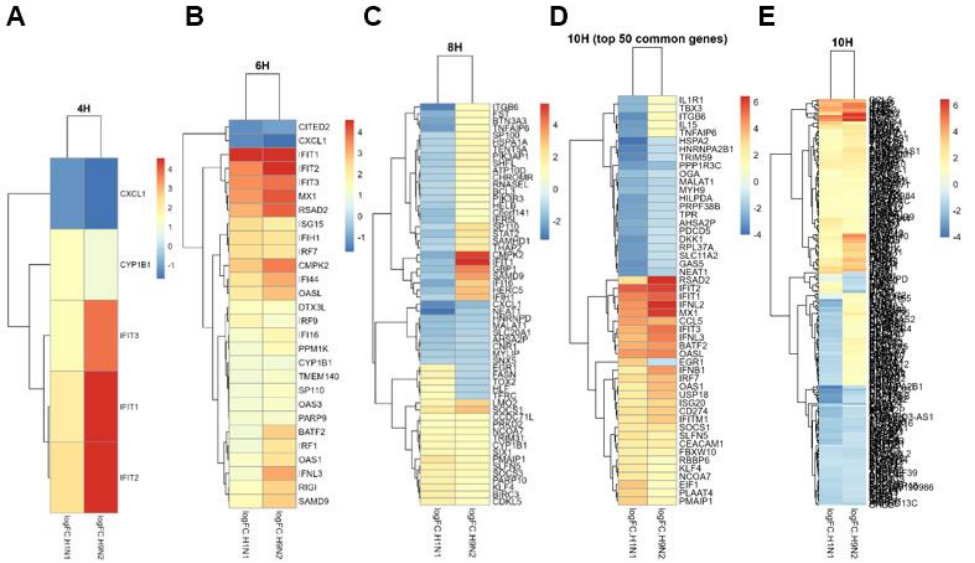

Figure 2. Heatmap of DEGs in A459 cells infected with H1N1/WSN, and H9N2 strains. **A:** Heatmap at 4 hpi. **B:** Heatmap at 6 hpi. **C:** Heatmap at 8 hpi. **D:** Heatmap at 10 hpi with top 50 lowest P-val. **E:** Heatmap at 10 hpi.

In Fig 2., heatmap analysis was utilized to visually represent the expression profiles of common differentially expressed genes (DEGs) between H1N1/WSN and H9N2 influenza strains across multiple time points (4, 6, 8, and 10 hours post-infection). Initial findings indicated consistent expression patterns (both up and downregulated) for common DEGs during the earlier phases up to 6 hours post-infection. However, as the infection progressed to 8 hours, divergences began to appear with certain genes such as CMPK2, IFIT1, GBP1, and SAMD9 exhibiting opposite regulation trends between the two viral strains. By the 10-hour mark, a subset of 192 common DEGs was identified, with the 50 genes displaying the most statistically significant changes (based on lowest p-values) being selected for enhanced visualization in Fig 2D. This detailed mapping and temporal profiling provide critical insights into the dynamic and strain-specific host responses to these influenza viruses, highlighting potential targets for therapeutic intervention.

4.2. Volcano Plot Comparisons

The volcano plot (Fig 3.) reveals notable differences in the regulatory patterns elicited by these two strains. For H1N1/WSN, the data (Fig 3A.) shows a relatively balanced response with comparable numbers of genes being upregulated and downregulated. In contrast, the H9N2 infection in Fig 3B. primarily results in a higher number of upregulated genes compared to downregulated ones. This could imply that H9N2 may trigger a more aggressive or unbalanced host response, potentially leading to excessive inflammatory responses or other pathological processes. Such a pattern of mostly upregulated genes suggests that H9N2 might be manipulating the host's cellular pathways more extensively to favor viral replication and spread, or alternatively, that the host's defensive response is more pronounced against this strain.

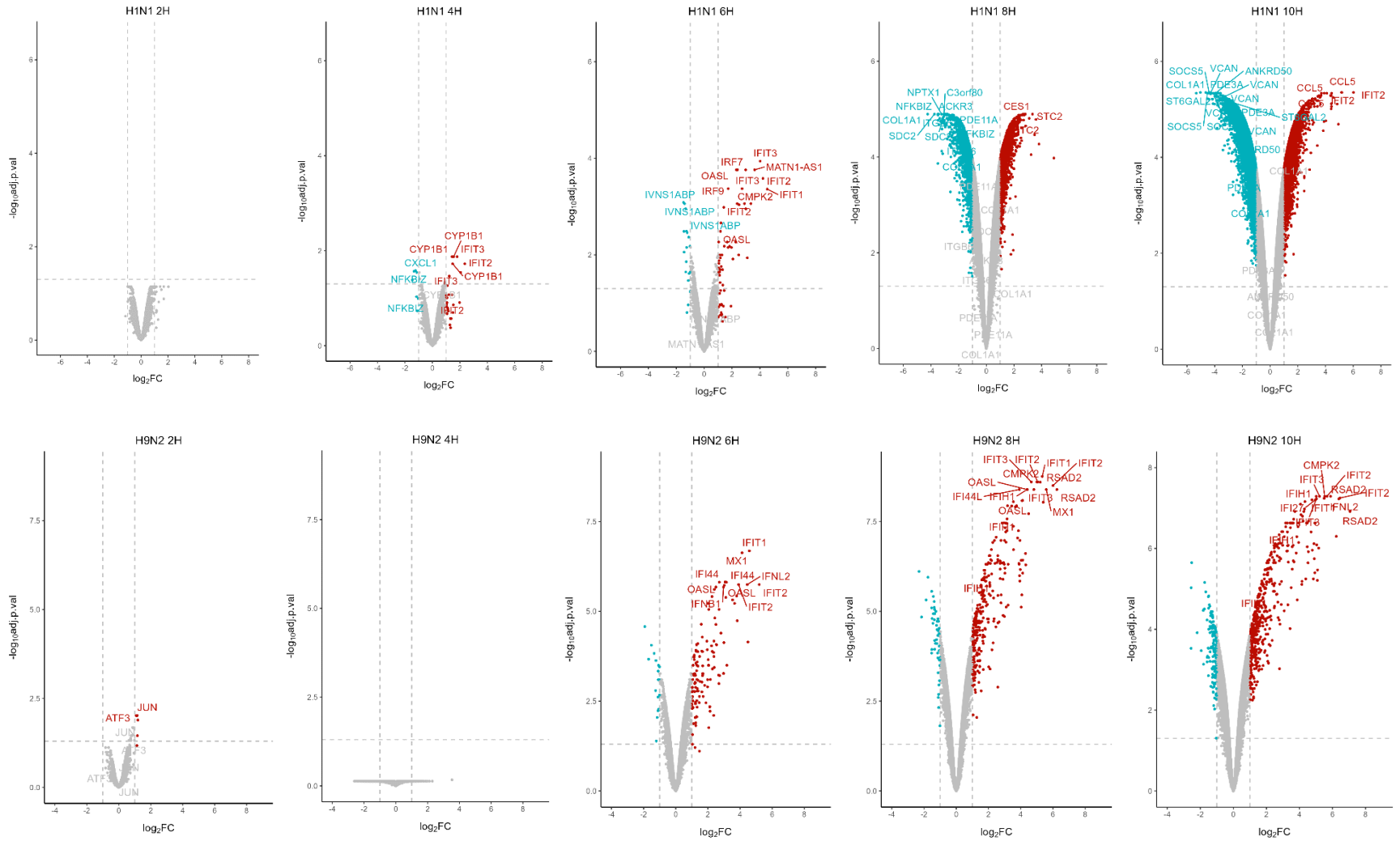

Figure 3. Volcano plot of 2,4,6,8,10 hpi. **A:** A549 cells infected with H1N1/WSN. **B:** A549 cells infected with H9N2. The x-axis (log2 fold change) displays the magnitude of expression change, indicating whether genes are upregulated (positive values) or downregulated (negative values) relative to control uninfected cells. The y-axis (-log10 p-value) represents the statistical significance of the expression changes, with higher values denoting lower p-values and thus more statistically significant differences. Points above the horizontal line indicate genes that meet the significance threshold (p-value < 0.05), and those to the right or left of the vertical lines meet the log fold change criterion (>|1|), highlighting genes considered significantly upregulated or downregulated.

4.3. Common DEGs Pathway Analysis

The common differentially expressed genes (DEGs) between H1N1/WSN and H9N2 influenza infections were analyzed to identify shared biological pathways activated or suppressed by these viruses. The number of common DEGs are shown in the Venn diagram below (Fig 4.). 112 genes were found to be upregulated and 80 genes downregulated in both conditions. These overlapping DEGs were then subjected to pathway analysis, which helped to uncover critical biological processes and molecular functions commonly influenced by both strains.

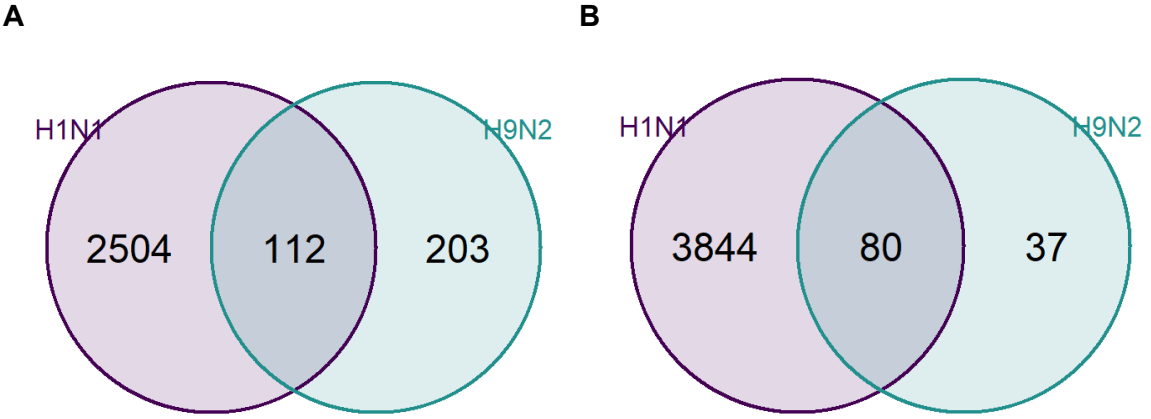

Figure 4. Venn diagram of number of DEGs infected with H1N1/WSN (purple), and H9N2 (green). **A:** Upregulated genes at 10 hpi. **B:** Downregulated genes at 10 hpi.

Table 3. identifies gene sets involved in the immune response to viral infections, pinpointing processes crucial for combating viruses such as Influenza A (H1N1/WSN) and H9N2. Key pathways include 'response to virus' with 46 genes including BST2 and MX1 highlighting the robust activation of antiviral defense mechanisms. Similarly, 'defense response to virus' and 'defense response to symbiont' pathways encompass a broad spectrum of interferon-stimulated genes (ISGs) that mediate cellular resistance to viral replication. Table 4. lists functions primarily associated with cytokine activity and RNA binding—critical roles in immune signaling and viral genome recognition. It features genes like IFIH1 and OAS1, which bind to viral RNA, disrupting viral replication. The identification of numerous cytokine activities, including those linked to inflammation and immune recruitment, underscores the cellular strategies to mitigate viral effects and signal distress.

Term[1]	Description[2]	Count[3]	adj.p.val[4]	Genes
GO:0009615	response to virus	46	5.21E-47	BST2; CCL5; CXCL10; DTX3L; GATA3; GBP3; HERC5; IFI16; IFI27; IFI44; IFI6; IFIH1; IFIT1; IFIT2; IFIT3; IFITM1; IFITM2; IFITM3; IFNB1; IFNL1; IFNL2; IFNL3; IRF1; IRF7; IRF9; ISG15; ISG20; LGALS9; MX1; MX2; MYD88; NT5C3A; OAS1; OAS2; OASL; PARP9; PLSCR1; PMAIP1; RIGI; RSAD2; SAMHD1; TLR3; TRIM25; TRIM31; ZBP1; ZC3HAV1;
GO:0051607	defense response to virus	42	1.27E-46	BST2; CXCL10; DTX3L; GBP3; HERC5; IFI16; IFI27; IFI6; IFIH1; IFIT1; IFIT2; IFIT3; IFITM1; IFITM2; IFITM3; IFNB1; IFNL1; IFNL2; IFNL3; IRF1; IRF7; IRF9; ISG15; ISG20; MX1; MX2; MYD88; NT5C3A; OAS1; OAS2; OASL; PARP9; PLSCR1; PMAIP1; RIGI; RSAD2; SAMHD1; TLR3; TRIM25; TRIM31; ZBP1; ZC3HAV1;
GO:0140546	defense response to symbiont	42	1.27E-46	BST2; CXCL10; DTX3L; GBP3; HERC5; IFI16; IFI27; IFI6; IFIH1; IFIT1; IFIT2; IFIT3; IFITM1; IFITM2; IFITM3; IFNB1; IFNL1; IFNL2; IFNL3; IRF1; IRF7; IRF9; ISG15; ISG20; MX1; MX2; MYD88; NT5C3A; OAS1; OAS2; OASL; PARP9; PLSCR1;

				PMAIP1; RIGI; RSAD2; SAMHD1; TLR3; TRIM25; TRIM31; ZBP1; ZC3HAV1;
GO:0045071	negative regulation of viral genome replication	19	1.35E-27	BST2; CCL5; IFI16; IFIH1; IFIT1; IFITM1; IFITM2; IFITM3; IFNB1; IFNL3; ISG15; ISG20; MX1; OAS1; OAS2; OASL; PLSCR1; RSAD2; ZC3HAV1;
GO:0048525	negative regulation of viral process	21	6.78E-27	BST2; CCL5; IFI16; IFIH1; IFIT1; IFITM1; IFITM2; IFITM3; IFNB1; IFNL3; ISG15; ISG20; MX1; OAS1; OAS2; OASL; PLSCR1; RSAD2; TRIM25; TRIM31; ZC3HAV1;
GO:1903900	regulation of viral life cycle	22	4.77E-24	BST2; CCL5; IFI16; IFIH1; IFIT1; IFITM1; IFITM2; IFITM3; IFNB1; IFNL3; ISG15; ISG20; LGALS9; MX1; OAS1; OAS2; OASL; PLSCR1; RSAD2; TRIM25; TRIM31; ZC3HAV1;
GO:0045069	regulation of viral genome replication	19	8.75E-24	BST2; CCL5; IFI16; IFIH1; IFIT1; IFITM1; IFITM2; IFITM3; IFNB1; IFNL3; ISG15; ISG20; MX1; OAS1; OAS2; OASL; PLSCR1; RSAD2; ZC3HAV1;
GO:0050792	regulation of viral process	22	9.69E-23	BST2; CCL5; IFI16; IFIH1; IFIT1; IFITM1; IFITM2; IFITM3; IFNB1; IFNL3; ISG15; ISG20; LGALS9; MX1; OAS1; OAS2; OASL; PLSCR1; RSAD2; TRIM25; TRIM31; ZC3HAV1;
GO:0019079	viral genome replication	20	6.35E-22	BST2; CCL5; IFI16; IFI27; IFIH1; IFIT1; IFITM1; IFITM2; IFITM3; IFNB1; IFNL3; ISG15; ISG20; MX1; OAS1; OAS2; OASL; PLSCR1; RSAD2; ZC3HAV1;
GO:0140888	interferon-mediated signaling pathway	18	7.50E-21	IFI27; IFITM1; IFITM2; IFITM3; IFNB1; IFNL1; IFNL2; IFNL3; IRF1; IRF7; ISG15; MYD88; OAS1; OAS2; PARP9; SAMHD1; USP18; ZBP1;

Table 3. GO biological process for upregulated DEGs. [1]Unique identifier for the Gene Ontology (GO) term associated with the listed biological processes. [2]The name of the biological process as described in the Gene Ontology database. [3]The number of differentially expressed genes (DEGs) associated with each GO term. [4]The P-value adjusted for multiple hypothesis testing using methods like the Benjamini-Hochberg methods [14], indicating the statistical significance of the enrichment of the DEGs in the respective GO term.

Term[1]	Description[2]	Count[3]	adj.p.val[4]	Genes
GO:0003725	double-stranded RNA binding	7	3.50E-05	IFIH1/OAS1/OAS2/OASL/RIGI/TLR3/ZBP1
GO:0005125	cytokine activity	8	0.006868	CCL5/CXCL10/CXCL11/IFNB1/IFNL1/IFNL2/IFNL3/TNFSF10
GO:0140297	DNA-binding transcription factor binding	11	0.006868	CREM/DLL1/DTX3L/GATA3/IFI27/KLF4/LMO2/NCOA7/OASL/PARP10/PARP9
GO:0008970	phospholipase A1 activity	3	0.006868	PLA2G4C/PLAAT2/PLAAT4
GO:0005126	cytokine receptor binding	8	0.006868	CCL5/CXCL10/CXCL11/GATA3/IFNB1/IFNL1/MYD88/TNFSF10
GO:0061629	RNA polymerase II-specific DNA-binding transcription factor binding	9	0.006868	DLL1/DTX3L/GATA3/IFI27/KLF4/LMO2/NCOA7/OASL/PARP9
GO:0016779	nucleotidyltransferase activity	6	0.008211	OAS1/OAS2/PARP10/PARP12/PARP9/TENT5A
GO:0003950	NAD+ ADP-ribosyltransferase activity	3	0.008211	PARP10/PARP12/PARP9
GO:1990404	NAD+-protein ADP-ribosyltransferase activity	3	0.008211	PARP10/PARP12/PARP9
GO:0070566	adenylyltransferase activity	3	0.01646	OAS1/OAS2/TENT5A

Table 4. GO molecular function for upregulated DEGs. [1]Unique identifier for the Gene Ontology (GO) term associated with the listed molecular functions. [2]The name of the molecular function as described in the Gene Ontology database. [3]The number of differentially expressed genes (DEGs) associated with each GO term. [4]The P-value adjusted for multiple hypothesis testing using methods like the Benjamini-Hochberg methods [14], indicating the statistical significance of the enrichment of the DEGs in the respective GO term.

In this study, the KEGG pathway analysis (Table 5.) revealed a significant correlation with the Hepatitis C. It has been reported that previous exposure to Influenza A might prepare the immune system to respond to Hepatitis C virus [21]. This finding suggests that the host cellular response mechanisms to these influenza infections share common pathways with those triggered by Hepatitis C virus infection. Such cross-pathway interactions highlight the intricate network of host-pathogen interactions and may provide insights into the broad-spectrum effects

of viral infections on human cells. Both COVID-19 and IAV viruses primarily target the respiratory tract, leading to a wide range of clinical manifestations, from mild respiratory symptoms to severe pneumonia and acute respiratory distress syndrome [22].

Term[1]	Description[2]	Count[3]	P-value	Genes
hsa05164	Influenza A	17	1.0E-14	OAS1; OAS2; CCL5; CXCL10; MX1; MX2; MYD88; RIGI; TNFSF10; IFNB1; IFIH1; IRF7; IRF9; RSAD2; SOCS3; TLR3; TRIM25;
hsa05160	Hepatitis C	13	3.9E-10	OAS1; OAS2; CXCL10; MX1; MX2; RIGI; IFNB1; IFIT1; IRF7; IRF9; RSAD2; SOCS3; TLR3;
hsa05169	Epstein-Barr virus infection	12	7.4E-8	OAS1; OAS2; CXCL10; ISG15; MYD88; RIGI; IFNB1; IRF7; IRF9; HLA-E; TAP1; TAP2;
hsa05162	Measles	10	2.8E-7	OAS1; OAS2; MX1; MX2; MYD88; RIGI; IFNB1; IFIH1; IRF7; IRF9;
hsa05171	Coronavirus disease	12	3.1E-7	OAS1; OAS2; CXCL10; ISG15; MX1; MX2; MYD88; RIGI; IFNB1; IFIH1; IRF9; TLR3;
hsa05168	Herpes simplex virus 1 infection	16	8.6E-7	OAS1; OAS2; CCL5; MYD88; RIGI; BST2; IFNB1; IFIH1; IRF7; IRF9; HLA-E; SOCS3; TLR3; TAP1; TAP2; ZNF596;
ko04623	Cytosolic DNA-sensing pathway	8	1.2E-6	CCL5; CXCL10; RIGI; SAMHD1; ZBP1; IFNB1; IFI16; IRF7;
map04620	Toll-like receptor signaling pathway	8	6.9E-6	CCL5; CXCL10; CXCL11; MYD88; IFNB1; IRF7; IRF9; TLR3;
map04622	RIG-I-like receptor signaling pathway	7	7.1E-6	CXCL10; ISG15; RIGI; IFNB1; IFIH1; IRF7; TRIM25;
hsa04621	NOD-like receptor signaling pathway	9	3.0E-5	OAS1; OAS2; CCL5; MYD88; GBP3; IFNB1; IFI16; IRF7; IRF9;

Table 5. Kyoto Encyclopedia of Genes and Genomes (KEGG) analysis for upregulated DEGs. [1]The biological classification system used to categorize the functional pathways in KEGG. [2]The name of the pathway as described in KEGG database. [3]The number of differentially expressed genes (DEGs) associated with each term.

Pathway	Term[1]	Description[2]	Count[3]	P-value	Genes
GO	GO:0010761	fibroblast migration	5	0.0048	AKAP12; IQGAP1; PLEC; THBS1; ZFAND5;
KEGG	hsa04350	TGF-beta signaling pathway	4	1.0E-2	ID2; THBS1; TFRC; TGFB2;

Table 6. Pathway analysis for downregulated in both H1N1/WSN and N9N2. [1]The biological classification system used to categorize the functional pathways; GO (Gene Ontology) or KEGG (Kyoto Encyclopedia of Genes and Genomes) [2]The biological process (for GO) or the signaling pathway (for KEGG) in which the downregulated genes are involved. [3]The number of differentially expressed genes (DEGs) associated with each term.

The pathway analysis for genes downregulated in both H1N1/WSN and H9N2 infections (Table 6.) has illuminated specific biological processes and signaling pathways adversely impacted by these viral infections. Notably, the gene ontology pathway analysis identified a reduction in genes associated with fibroblast migration, including AKAP12, IQGAP1, PLEC, THBS1, and ZFAND5. Similarly, the KEGG pathway analysis highlighted a downregulation in components of the TGF-beta signaling pathway, specifically ID2, THBS1, TFRC, and TGFB2. These insights into the downregulated pathways offer a deeper understanding of the complex interplay between the host cellular machinery and viral infection, potentially guiding the development of therapeutic strategies that can restore these vital cellular functions.

Detailed pathway analysis for each virus strains (H1N1/WSN and H9N2) are shown in the appendix. For H1N1/WSN infected A549 cell, KEGG upregulated pathway analysis showed ‘Dilated cardiomyopathy’, ‘MAPK signaling pathway’, ‘Type 2 diabetes mellitus’ whereas H9N2 had similar result to Table 5. For GO upregulated pathway analysis in H1N1/WSN, there were positive regulation of both cell adhesion and cell activation and H9N2 had similar result to Table 3.

4.4. Network Analysis

The network analysis of A549 cells infected with H1N1/WSN and H9N2 influenza viruses revealed distinct patterns of gene regulation over time. The networks at 6, 8, and 10 hours post-infection were characterized by a moderate number of upregulated (red) and downregulated (blue) genes (Fig 5.). Visual inspection of the networks highlighted the predominance of red nodes in the H9N2 networks, consistent across all observed time points, underscoring a persistent upregulation of immune and antiviral genes. In contrast, the H1N1/WSN networks exhibited a more balanced distribution of red and blue nodes.

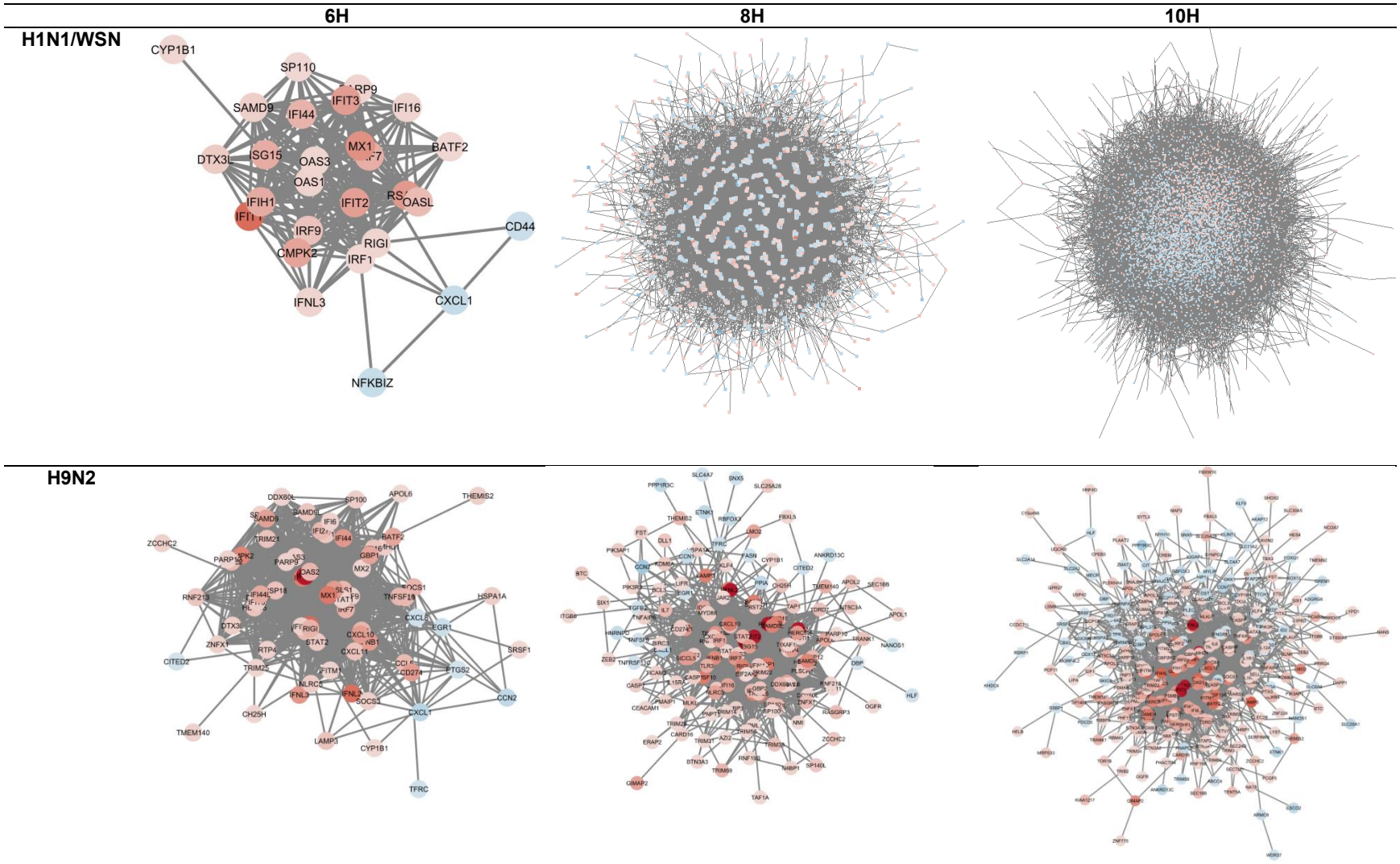

Figure 5. Gene Network Using Cytoscape [15]. Upregulated genes are shown in red, and downregulated genes are shown in blue.

4.5. Drug Prediction Using Hub Genes

The 10 upregulated hub genes identified in this study (Fig 6.)—DDX58, IFIT2, MX1, IFIH1, IRF1, OAS1, OAS2, ISG15, IRF7, and IFIT1—play pivotal roles in the innate immune response to viral infections [23]. DDX58 (RIG-I) and IFIH1 (MDA5) are critical for recognizing viral RNAs and initiating antiviral signaling pathways that activate interferon regulatory factors such as IRF3 and IRF7, leading to the production of type I interferons [23]. These interferons upregulate genes like IFIT1, IFIT2, and MX1, which further enhance the cellular antiviral state [23]. For instance, MX1 exerts its antiviral effects by inhibiting viral replication and assembly processes [23]. The widespread upregulation of these genes during H1N1/WSN and H9N2 infections highlights their essential role in mounting a robust antiviral response, underscoring their potential as targets for therapeutic interventions to modulate immune responses and improve outcomes in viral infections. These findings enrich the understanding of host-pathogen interactions and could guide the development of strategies to enhance antiviral defenses in respiratory epithelial cells.

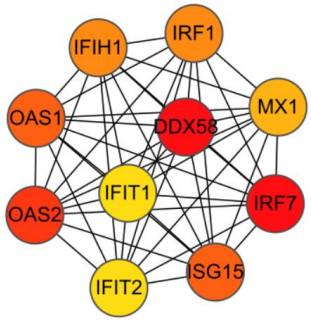

Figure 6. Upregulating hub genes with most degrees. Number of degrees were calculated using cytoHubba [18].

The drug target prediction analysis using the 10 upregulated hub genes (DDX58, IFIT2, MX1, IFIH1, IRF1, OAS1, OAS2, ISG15, IRF7, and IFIT1) identified several compounds with potential therapeutic implications for viral infections (Table 7.). These drugs were found to have significant interactions with the hub genes involved in the immune response against viruses, particularly in influenza A virus (H1N1/WSN, and H9N2) infections.

Name	Genes	adj.P.Val*
suloctidil HL60 UP	IFIH1; OAS1; DDX58; OAS2; IRF1; MX1; IRF7; ISG15; IFIT1; IFIT2;	6.29E-20
prenylamine HL60 UP	IFIH1; OAS1; DDX58; MX1; IRF7; ISG15; IFIT1; IFIT2	4.96E-19
terfenadine HL60 UP	IFIH1; OAS1; DDX58; MX1; IRF7; ISG15; IFIT1; IFIT2	1.73E-17
propofol MCF7 UP	IFIH1; OAS1; DDX58; IRF1; ISG15; IFIT1; IFIT2	5.97E-15
benfluorex MCF7 UP	IFIH1; OAS1; DDX58; IRF1; IFIT1; IFIT2	6.42E-14
prochlorperazine MCF7 UP	IFIH1; OAS1; DDX58; IRF7; ISG15; IFIT1	4.53E-12
etoposide HL60 UP	IFIH1; OAS1; DDX58; MX1; IRF7; ISG15; IFIT1	4.84E-12
acetohexamide PC3 UP	IFIH1; OAS1; OAS2; MX1; IFIT1	1.14E-11
3'-Azido-3'-deoxythymidine CTD 00007047	IFIH1; OAS1; OAS2; MX1; IRF7; ISG15; IFIT1; IFIT2	1.93E-11
chlorophyllin CTD 00000324	OAS1; OAS2; MX1; ISG15; IFIT1	3.85E-11

Table 7. Top 10 Drug candidates from upregulated hub genes. *The P-value adjusted for multiple hypothesis testing using Benjamini-Hochberg method [14].

Suloctidil HL60 UP and related compounds like Prenylamine HL60 UP and Terfenadine HL60 UP exhibited the strongest associations, with adjustment P-values reaching as low as 6.29E-20. These drugs mainly target genes integral to the antiviral response, including those encoding for proteins like RIG-I, MDA5, and the OAS family, which are crucial in the detection and response to viral RNA [24]. Propofol MCF7 UP, known for its role in anesthesia, also showed interaction

with antiviral genes such as DDX58 and IFIT proteins, suggesting potential off-target effects that could influence immune responses. Similarly, Benfluorex MCF7 UP and Prochlorperazine MCF7 UP interact with a subset of these genes, implicating their roles in modulating viral defense mechanisms [24]. Drugs like Etoposide HL60 UP and Acetohexamide PC3 UP, typically associated with cancer therapy and diabetes treatment respectively, were predicted to interact with these immune-related genes, possibly affecting viral replication and host viral defense mechanisms. The antiretroviral 3'-Azido-3'-deoxythymidine CTD 00007047 showed a broad spectrum of gene interactions, consistent with its known effects on viral processes [24]. Chlorophyllin CTD 00000324, a less common compound in viral therapeutics, was identified to interact with genes such as OAS1 and MX1, which might suggest new avenues for its use in enhancing antiviral responses [24].

5. Discussion

The DEG analysis helps identify critical time points and the extent of gene expression alterations, which can be pivotal for further studies focusing on therapeutic target identification and the development of intervention strategies against these infections. H1N1/WSN induces a significantly higher number of DEGs than H9N2 at later time points, suggesting that although H9N2 acts faster initially, H1N1/WSN might trigger more profound cellular alterations as the infection progresses. This might reflect differences in the viruses' strategies for evading immune detection and sustaining infection within host cells.

Throughout the timepoints analyzed, IFITs—particularly IFIT1 and IFIT2—have been consistently upregulated, serving dual roles both as antiviral agents and in functions beyond combating viruses. These proteins are effective against influenza viruses by inhibiting viral RNA synthesis and the activity of viral polymerase [25]. The study has revealed a similar upregulation in genes such as IFI6, IFIT2, ISG15, HERC5, RSAD2, IFIT3, IFITM1, and CXCL10 in response to infections by H1N1/WSN and H9N2 strains. These genes are crucial in enhancing the antiviral defenses of alveolar basal and airway epithelial cells against diverse influenza A virus strains [26]. Additionally, genes like IFITM3, OAS2, and MX1 have shown significant upregulation in epithelial cells affected by SARS-CoV-2, which underscores a potentially essential aspect of the cellular defense mechanism that may be commonly activated across various viral infections [27]. This finding suggests a shared antiviral response pathway among H1N1/WSN, H9N2 influenza viruses, and SARS-CoV-2.

The network analyses indicate distinctive responses triggered by H1N1/WSN and H9N2 infections. H1N1/WSN typically prompts a direct antiviral response, whereas H9N2 might engage more complex regulatory strategies, manipulating both upregulation and downregulation of pivotal gene groups. This complexity might reflect adaptive mechanisms by H9N2 to circumvent host defenses or modulate the host immune response more subtly. The consistent enrichment of interferon-stimulated genes (ISGs) like IFIH1, OAS1, and DDX58 in various drug screenings highlights a common pathway that is crucial for antiviral defense and implicated in autoimmune diseases [28, 29]. Understanding the interactions between specific drugs and these ISGs is essential for predicting drug efficacy and potential adverse reactions.

6. Conclusion

This study systematically analyzes transcriptomic changes induced by H1N1/WSN and H9N2 influenza virus infections in A549 cells, providing critical insights into cellular molecular interplay during infection. The findings delineate distinct and overlapping gene expression profiles prompted by these influenza subtypes, deepening understanding of their pathogenic mechanisms. Differential expression analysis pinpoints several potential therapeutic targets

involved in antiviral responses, notably within interferon signaling and viral replication pathways, suggesting new directions for antiviral strategy development.

Through detailed pathway and network analyses, the study identified significant changes in metabolic pathways and regulatory networks that are crucial during influenza virus infections. It was observed that both H1N1/WSN and H9N2 viruses initiate unique transcriptional modifications in the host cells, highlighting virus-specific and common molecular targets that could serve as potential points for therapeutic intervention. Particularly, the research highlighted shared pathways and key regulatory genes that are consistently altered across both viral infections, suggesting potential targets for broad-spectrum antiviral drugs.

Moreover, the study demonstrated that integrating advanced bioinformatics tools to analyze complex viral-host interactions enhances our understanding of disease mechanisms and can accelerate the identification of novel drug targets. The findings underscore the potential of using such integrative approaches to develop therapeutic strategies not only for influenza but also for other respiratory viral infections, thereby improving our preparedness and response capabilities against future outbreaks. This aligns with the study's objectives to bridge the gap between species-specific responses and universal treatment approaches, potentially leading to the development of effective universal antiviral agents.

7. References

[1] Garten RJ, Davis CT, Russell CA, Shu B, Lindstrom S, Balish A, et al. (2009). "Antigenic and genetic characteristics of swine-origin 2009 A(H1N1) influenza viruses circulating in humans." Science, 325(5937), 197-201. DOI:10.1126/science.1176225

[2] Peiris M, Yuen KY, Leung CW, Chan KH, Ip PL, Lai RW, et al. (1999). "Human infection with influenza H9N2." Lancet, 354(9182), 916-917. DOI:10.1016/S0140-6736(99)03311-5

[3] Taye B, Yeo, D., Lee, R.T.C., Tan, B.H., Sugrue, R.J., Maurer-Stroh, S. "Inter-Species Host Gene Expression Differences in Response to Human and Avian Influenza A Virus Strains." Int. J. Mol. Sci. 2017, 18, 2295. https://doi.org/10.3390/ijms18112295. ↩

[4] Taye B, Chen H, Yeo DS, Seah SG, Wong MS, Sugrue RJ, Tan BH. "A System Based-Approach to Examine Host Response during Infection with Influenza A Virus Subtype H7N9 in Human and Avian Cells." Cells. 2020 Feb 15;9(2):448. https://doi.org/10.3390/cells9020448. ↩

[5] Casamassimi A, Federico A, Rienzo M, Esposito S, Ciccodicola A. Transcriptome Profiling in Human Diseases: New Advances and Perspectives. Int J Mol Sci. 2017;18(8):1652. Published 2017 Jul 29. doi:10.3390/ijms18081652

[6] Schenone M, Dančík V, Wagner BK, Clemons PA. Target identification and mechanism of action in chemical biology and drug discovery. Nat Chem Biol. 2013;9(4):232-240. doi:10.1038/nchembio.1199

[7] Carterson AJ, Höner zu Bentrup K, Ott CM, et al. A549 lung epithelial cells grown as three-dimensional aggregates: alternative tissue culture model for Pseudomonas aeruginosa pathogenesis. Infect Immun. 2005;73(2):1129-1140. doi:10.1128/IAI.73.2.1129-1140.2005

[8] Sutejo R, Yeo DS, Myaing MZ, et al. Activation of type I and III interferon signalling pathways occurs in lung epithelial cells infected with low pathogenic avian influenza viruses. PLoS One. 2012;7(3):e33732. doi:10.1371/journal.pone.0033732

[9] Gautier L, Cope L, Bolstad BM, Irizarry RA (2004). “affy—analysis of Affymetrix GeneChip data at the probe level.” Bioinformatics, 20(3), 307–315. ISSN 1367-4803, doi:10.1093/bioinformatics/btg405.

[10] Ritchie ME, Phipson B, Wu D, et al. limma powers differential expression analyses for RNA-sequencing and microarray studies. Nucleic Acids Res. 2015;43(7):e47. doi:10.1093/nar/gkv007

[11] The Gene Ontology Consortium. The Gene Ontology knowledgebase in 2023. Genetics. 2023 May 4;224(1):iyad031. DOI: 10.1093/genetics/iyad031

[12] Kanehisa M, Goto S. KEGG: kyoto encyclopedia of genes and genomes. Nucleic Acids Res. 2000;28(1):27-30. doi:10.1093/nar/28.1.27

[13] Yu G, Wang LG, Han Y, He QY. clusterProfiler: an R package for comparing biological themes among gene clusters. OMICS. 2012;16(5):284-287. doi:10.1089/omi.2011.0118

[14] Haynes, W. (2013). Benjamini–Hochberg Method. In: Dubitzky, W., Wolkenhauer, O., Cho, KH., Yokota, H. (eds) Encyclopedia of Systems Biology. Springer, New York, NY. https://doi.org/10.1007/978-1-4419-9863-7_1215

[15] Shannon P, Markiel A, Ozier O, et al. Cytoscape: a software environment for integrated models of biomolecular interaction networks. Genome Res. 2003;13(11):2498-2504. doi:10.1101/gr.1239303

[16] Szklarczyk D, Kirsch R, Koutrouli M, et al. The STRING database in 2023: protein-protein association networks and functional enrichment analyses for any sequenced genome of interest. Nucleic Acids Res. 2023;51(D1):D638-D646. doi:10.1093/nar/gkac1000

[17] Yu D, Lim J, Wang X, Liang F, Xiao G. Enhanced construction of gene regulatory networks using hub gene information. BMC Bioinformatics. 2017;18(1):186. Published 2017 Mar 23. doi:10.1186/s12859-017-1576-1

[18] Chin CH, Chen SH, Wu HH, Ho CW, Ko MT, Lin CY. cytoHubba: identifying hub objects and sub-networks from complex interactome. BMC Syst Biol. 2014;8 Suppl 4(Suppl 4):S11. doi:10.1186/1752-0509-8-S4-S11

[19] Kuleshov MV, Jones MR, Rouillard AD, et al. Enrichr: a comprehensive gene set enrichment analysis web server 2016 update. Nucleic Acids Res. 2016;44(W1):W90-W97. doi:10.1093/nar/gkw377

[20] Yoo M, Shin J, Kim J, et al. DSigDB: drug signatures database for gene set analysis. Bioinformatics. 2015;31(18):3069-3071. doi:10.1093/bioinformatics/btv313

[21] Wedemeyer H, Mizukoshi E, Davis AR, Bennink JR, Rehermann B. Cross-reactivity between hepatitis C virus and Influenza A virus determinant-specific cytotoxic T cells. J Virol. 2001;75(23):11392-11400. doi:10.1128/JVI.75.23.11392-11400.2001

[22] Flerlage T, Boyd DF, Meliopoulos V, Thomas PG, Schultz-Cherry S. Influenza virus and SARS-CoV-2: pathogenesis and host responses in the respiratory tract. Nat Rev Microbiol. 2021;19(7):425-441. doi:10.1038/s41579-021-00542-7

[23] The GeneCards Suite: From Gene Data Mining to Disease Genome Sequence Analyses (PMID: 27322403; Citations: 3,096)
Stelzer G, Rosen R, Plaschkes I, Zimmerman S, Twik M, Fishilevich S, Iny Stein T, Nudel R, Lieder I, Mazor Y, Kaplan S, Dahary, D, Warshawsky D, Guan - Golan Y, Kohn A, Rappaport N, Safran M, and Lancet D

[24] Yoo M*, Shin J*, Kim J, Ryall KA, Lee K, Lee S, Jeon M, Kang J, Tan AC. (2015). DSigDB: Drug Signatures Database for Gene Set Analysis. ***Bioinformatics.*** 31(18): 3069-3071. [PMID: 25990557].

[25] Zhu Z, Yang X, Huang C, Liu L. The Interferon-Induced Protein with Tetratricopeptide Repeats Repress Influenza Virus Infection by Inhibiting Viral RNA Synthesis. Viruses. 2023; 15(7):1412. https://doi.org/10.3390/v15071412

[26] Zhou A, Dong X, Liu M, Tang B. Comprehensive Transcriptomic Analysis Identifies Novel Antiviral Factors Against Influenza A Virus Infection. Front Immunol. 2021;12:632798. Published 2021 Jul 21. doi:10.3389/fimmu.2021.632798

[27] Hachim MY, Al Heialy S, Hachim IY, et al. Interferon-Induced Transmembrane Protein (IFITM3) Is Upregulated Explicitly in SARS-CoV-2 Infected Lung Epithelial Cells. Front Immunol. 2020;11:1372. Published 2020 Jun 10. doi:10.3389/fimmu.2020.01372

[28] Rice GI, Del Toro Duany Y, Jenkinson EM, et al. Gain-of-function mutations in IFIH1 cause a spectrum of human disease phenotypes associated with upregulated type I interferon signaling. Nat Genet. 2014;46(5):503-509. doi:10.1038/ng.2933

[29] Wong, MT., Chen, SL. Emerging roles of interferon-stimulated genes in the innate immune response to hepatitis C virus infection. Cell Mol Immunol 13, 11–35 (2016). https://doi.org/10.1038/cmi.2014.127

Acknowledgments

The author wishes to express sincere gratitude to Associate professor Tan Boon Huan and Associate Professor Sourav Saha Bhowmick, who provided invaluable guidance and expert knowledge throughout the research and writing process of this paper. Their insights and suggestions were crucial in shaping both the analytical framework and the direction of the study.

Appendix

H1N1/WSN Upregulated DEGs Pathway Analysis

H1N1/WSN Upregulated

KEGG Pathway	Count	P-Value	Genes
Dilated cardiomyopathy	31	2.2E-06	ATP2A2; ATP2A3; GNAS; ADCY1; ADCY2; ADCY5; ADCY9; CACNG2; CACNG3; CACNG6; CACNG7; CACNG8; CACNA1C; CACNA1D; DES; DTNA; IGF1; ITGA2B; ITGA7; ITGA8; ITGA9; ITGB4; LMNA; LAMA2; MYH6; MYL3; SSPN; SLC8A1; SNTB2; TGFB2; TNNC1;
MAPK signaling pathway	63	1.0E-05	AKT2; DDIT3; JUN; JUND; KIT; MECOM; MYD88; RAP1A; RASGRP2; RAC2; AREG; ARRB2; CACNG2; CACNG3; CACNG6; CACNG7; CACNG8; CACNA1A; CACNA1B; CACNA1C; CACNA1D; CACNA1G; CACNA1H; CACNA1I; DUSP6; DUSP9; EFNA2; EREG; ERBB4; FGF18; FGF21; FGF22; FGF3; FGF4; FGF8; FLT4; GADD45A; Hsp70; HSPA6; IGF1; IGF2; INS; MAPK1; MAPK10; MAPK11; MAPK13; MAPK8IP2; MAPK8IP3; MAP2K3; MAP2K7; MAP3K13; NTRK1; NTF3; NFKB2; PSPN; PLA2G4C; PLA2G4F; PDGFRB; PDGFB; PRKCG; PTPN5; RPS6KA4; TGFA; TGFB2;
Type Ⅱ diabetes mellitus	17	4.9E-05	ABCC8; CACNA1A; CACNA1B; CACNA1C; CACNA1D; CACNA1G; HK3; INS; MAPK1; MAPK10; PDX1; KCNJ11; PRKCE; PRKCZ; PKLR; SOCS1; SOCS3
Adrenergic signaling in cardiomyocytes	37	5.2E-05	AKT2; ATP1B3; ATP2A2; ATP2A3; BCL2; GNAI2; GNAS; RAPGEF3; ADCY1; ADCY2; ADCY5; ADCY9; ADRA1A; CREM; CACNG2; CACNG3; CACNG6; CACNG7; CACNG8; CACNA1C; CACNA1D; CAMK2B; CAMK2D; CALML5; MAPK1; MAPK11; MAPK13; MYH6; MYL3; LOC102723475; PPP1R1A; PPP2CB; PPP2R3B; PPP2R5A; PPP2R2C; SLC8A1; TNNC1;
Cell adhesion molecules	37	9.1E-05	CD22; CD274; CD99; LOC102723996; PVR; VSIR; CDH15; CDH4; CLDN1; CLDN11; CLDN16; CLDN5; CLDN7; CNTN1; CNTN2; ICOS; ITGA8; ITGA9; ITGB2; ICAM2; LRRC4B; LRRC4C; HLA-E; HLA-DOA; HLA-DPB1; HLA-DQB1; HLA-DRB1; MAG; NTNG2; NRXN1; NRXN2; NLGN2; PECAM1; PDCD1; PTPRS; SPN; SDC4;

H1N1/WSN Upregulated

GO Enrichment Analysis	GO ID	Count	P-Value	Genes

Positive regulation of cell adhesion	GO:0045785	105	2.99E-11	CCL5; CEACAM6; PRKCE; UNC13D; SOCS1; RUNX1; CD274; IL4I1; BCL6; TFRC; RREB1; FBLN2; CD44; CDK6; HSPH1; SLC7A1; PRSS2; FCHO1; SFRP1; IL1RL2; ALOX5; JAK3; AGER; FLCN; HLA-DRB1; ITGB1BP1; SMARCD3; SHH; AGR2; FOXA2; SMARCA4; SOX4; ADAM8; CCN1; GATA3; RHOD; SPOCK2; PYCARD; AZU1; CYTH3; FOXO3; THY1; FOXP3; ITGB2; FUT1; HLA-DOA; LIMS2; IHH; IGF2; ZFHX3; ROCK1; ZAP70; TFE3; EFNB2; IL12RB1; LEF1; SRC; ADAM9; LGALS9; LAMA2; VSIR; ITPKB; HLA-E; CD55; CR1; EPB41L4B; IL6ST; PRKD2; IGF1; PTPN23; ADAM19; WNT4; RUNX3; PDGFB; CITED2; TNFSF14; CHRD; SART1; FUT3; PRKCZ; EPHA1; ELANE; ICOS; EMILIN2; DOCK1; TGFB2; HLA-DQB1; CD74; EFNB1; ACTL6B; SDC4; HLA-DQB2; FGB; NCKAP1L; EBI3; HLA-DPB1; ICOSLG; AMBRA1; RAG1; SMARCA2; TNFRSF14; STX4; ZMIZ1; VTN; FGG;
Positive regulation of cell activation	GO:0050867	86	1.68E-09	CCL5; JUND; BCL2; SOCS1; RUNX1; CD274; IL4I1; BCL6; TFRC; TYROBP; VAMP8; HSPH1; SLC7A1; FCHO1; IL1RL2; JAK3; AGER; HLA-DRB1; KMT5C; SMARCD3; SHH; LILRA2; SMARCA4; SOX4; ADAM8; GATA3; PYCARD; FOXO3; THY1; FOXP3; ITGB2; SPACA3; HLA-DOA; SPI1; IHH; BLOC1S3; GATA1; IGF2; ZAP70; EFNB2; IL12RB1; LEF1; SRC; LGALS9; LILRA5; MYD88; TLR9; VSIR; INPP5D; ITPKB; HLA-E; KLRC2; CD55; GATA2; CR1; IL6ST; IGF1; PDGFRB; CD38; ITGAM; RUNX3; HAMP; CAPN3; TNFSF14; TNFRSF4; SART1; PRKCZ; ICOS; HLA-DQB1; CD74; EFNB1; ACTL6B; HLA-DQB2; CHRNB2; NCKAP1L; EBI3; HLA-DPB1; ICOSLG; AMBRA1; RAG1; SMARCA2; CCN2; TNFRSF14; STX4; ZMIZ1; MMP14;
Defense response to virus	GO:0051607	71	1.93E-09	IFIT2; OASL; IFIT3; IFNL2; IFNL3; RSAD2; PMAIP1; MX1; IFIT1; IRF7; BCL2; IFITM1; IFNB1; UNC13D; TRIM8; OAS1; ISG20; ADARB1; IFNL1; ISG15; IFIH1; NT5C3A; PARP9; RIOK3; IFI27; VAMP8; IRF9; ZBP1; TRIM25; IFITM3; DTX3L; ZC3HAV1; PLA2G10; IRF1; DEFA1; DHX58; IFI6; IFITM2; PYCARD; AZU1; FOXP3; PLSCR1; EXOSC4; TRIM31; ARMC5; IL12RB1; RIGI; PRF1; PTPRS; MYD88; TLR9; BST2; NLRP1; UNC93B1; ZDHHC1; SAMHD1; CXCL10; PDE12; OAS2; ATAD3A; ZCCHC3; BCL2L1; POLR3E; IFI16; DDIT4; TLR3; GBP3; NLRP6; HERC5; SEC14L1; MX2;
Response to virus	GO:0009615	88	2.02E-09	CCL5; IFIT2; OASL; IFIT3; IFNL2; IFNL3; RSAD2; PMAIP1; MX1; IFIT1; IRF7; BCL2; IFITM1; IFNB1; UNC13D; TRIM8; OAS1; ISG20; ADARB1; IFNL1; ISG15; IFIH1; NT5C3A; PARP9; CDK6; ARF1; RIOK3; IFI27; VAMP8; IRF9; ZBP1; TRIM25; IFITM3; DTX3L; ZC3HAV1; PLA2G10; RPS15A; H19; IRF1; GATA3; DEFA1; DHX58; IFI6; POU2F2; IFITM2; PYCARD; AZU1; MAPK11; IFI44; FOXP3; ODC1; PLSCR1; EXOSC4; TRIM31; ARMC5; IL12RB1; CLU; SRC; RIGI; PRF1; EIF5A; LGALS9; PTPRS; BTBD17; MYD88; TLR9; BST2; NLRP1; UNC93B1; ZDHHC1; DDX3X; SAMHD1; CXCL10; PDE12; OAS2; ATAD3A; ZCCHC3; BCL2L1; POLR3E; IFI16; DDIT4; TLR3; GBP3; NLRP6; HERC5; SEC14L1; MX2; CXCR4;
Defense response to symbiont	GO:0140546	71	2.25E-09	IFIT2; OASL; IFIT3; IFNL2; IFNL3; RSAD2; PMAIP1; MX1; IFIT1; IRF7; BCL2; IFITM1; IFNB1; UNC13D; TRIM8; OAS1; ISG20; ADARB1; IFNL1; ISG15; IFIH1; NT5C3A; PARP9; RIOK3; IFI27; VAMP8; IRF9; ZBP1; TRIM25; IFITM3; DTX3L; ZC3HAV1; PLA2G10; IRF1; DEFA1; DHX58; IFI6; IFITM2; PYCARD; AZU1; FOXP3; PLSCR1; EXOSC4; TRIM31; ARMC5; IL12RB1; RIGI; PRF1; PTPRS; MYD88; TLR9; BST2; NLRP1; UNC93B1; ZDHHC1; SAMHD1; CXCL10; PDE12; OAS2; ATAD3A; ZCCHC3; BCL2L1; POLR3E; IFI16; DDIT4; TLR3; GBP3; NLRP6; HERC5; SEC14L1; MX2;

H1N1/WSN Downregulated DEGs Pathway Analysis

H1N1/WSN Downregulated

KEGG Pathway	Count	P-Value	Genes

Cell cycle	64	3.5E-10	ABL1; ATM; ATR; ATRX; BUB1B; BUB1; CREBBP; DBF4B; DDX11; E2F5; FBXO5; MAU2; MDM2; NDC80; NIPBL; PDS5B; RBL1; RBL2; SKP2; SMAD2; SMAD3; SMAD4; TICRR; TTK; WEE1; ANAPC1; ANAPC4; ANAPC5; ANAPC7; AURKB; CDC16; CDC23; CDC25A; CDC25C; CDC6; CDC7; CHEK1; CDT1; CCNA2; CCNB1; CCND1; CCNE1; CCNE2; CDK1; CDK6; ESCO1; ESCO2; ESPL1; KNL1; MCM4; MCM5; MCM6; MAD1L1; MAD2L1; ORC1; ORC2; ORC4; PLK1; PCNA; PRKDC; PPP2R1B; TFDP2; TGFB1; TGFB2;
TGF-beta signaling pathway	44	2.9E-07	CREBBP; E2F5; RBL1; SIN3A; SKIL; SKI; SMAD1; SMAD2; SMAD3; SMAD4; SMAD5; SMAD7; SMURF1; SMURF2; SP1; ACVR1; ACVR1B; ACVR2A; ACVR2B; BMP2; BMP6; BMPR1A; BMPR1B; BMPR2; FST; HFE; INHBC; ID1; ID2; ID3; ID4; LTBP1; MAPK1; NCOR1; PPP2R1B; RPS6KB1; THBS1; THSD4; TFRC; TGFB1; TGFB2; TGFBR1; TGFBR2; ZFYVE16;
Hepatocellular carcinoma	58	2.0E-06	AKT3; APC; ARID1A; ARID1B; ARID2; BRAF; POLK; ELK1; FRAT2; GAB1; LRP5; LRP6; PHF10; SMAD2; SMAD3; SMAD4; SOS1; SOS2; SMARCC1; SMARCC2; SMARCA2; SMARCD1; SMARCD3; WNT5A; AXIN2; CSNK1A1; CTNNB1; CCND1; CDK6; DVL2; DVL3; EGFR; FZD1; FZD2; FZD3; FZD5; FZD7; FZD8; HMOX1; IGF1R; KEAP1; MGST1; MAPK1; PTEN; PIK3CA; PIK3CB; PIK3R3; PLCG1; PLCG2; PBRM1; PRKCA; RPS6KB1; TCF7L2; TCF7; TGFB1; TGFB2; TGFBR1; TGFBR2;
FoxO signaling pathway	47	7.0E-06	AKT3; ATM; BRAF; BCL2L11; C8orf44-SGK3; CREBBP; FBXO32; MDM2; RBL2; SKP2; SMAD3; SMAD4; SOS1; SOS2; CCNB1; CCND1; CCNG2; EGFR; FOXO1; FOXO3; HOMER1; IKBKB; IGF1R; IRS1; INSR; MAPK1; MAPK12; MAPK8; MAPK9; NLK; PTEN; PIK3CA; PIK3CB; PIK3R3; PLK1; PLK4; PRKAA1; PRKAA2; PRKAB2; STK4; SGK1; SIRT1; SOD2; TGFB1; TGFB2; TGFBR1; TGFBR2;
Signaling pathways regulating pluripotency of stem cells	50	7.7E-06	AKT3; APC; JAK1; LIF; REST; SKIL; SMAD1; SMAD2; SMAD3; SMAD4; SMAD5; SMARCAD1; TBX3; WNT5A; ACVR1; ACVR1B; ACVR2A; ACVR2B; AXIN2; BMPR1A; BMPR1B; BMPR2; CTNNB1; DVL2; DVL3; FGFR1; FZD1; FZD2; FZD3; FZD5; FZD7; FZD8; INHBC; ID1; ID2; ID3; ID4; IGF1R; JARID2; KAT6A; MAPK1; MAPK12; PIK3CA; PIK3CB; PIK3R3; PCGF1; PCGF3; RIF1; TCF7; ZFHX3;

H1N1/WSN Downregulated

GO Enrichment Analysis	GO ID	Count	P-Value	Genes
Histone modification	GO:0016570	181	7.72E-23	NCOA3; SETD5; KDM4B; BRD8; KDM2B; BOD1L1; KAT6B; SFPQ; DYRK1A; OGT; KDM3A; RIOX1; SIN3A; GTF2B; MLLT10; RIF1; TADA1; RNF168; KDM5D; MEN1; AUTS2; SIRT1; MTF2; ASH1L; HASPIN; KANSL2; NFKBIZ; NNMT; SETMAR; HDAC4; TAF5; UBR5; KDM5B; NAA40; MBTD1; KMT2A; KDM5A; KMT2D; USP21; BEND3; JARID2; BAP1; LRRK2; RBM14; KMT2C; TRRAP; PRDM2; SF3B3; KDM3B; MTHFR; KAT7; SREBF1; ASXL1; WDR5B; JMJD1C; RCOR3; JADE1; RTF1; NIPBL; EED; UBR2; ATXN7; EHMT1; VCPKMT; CHTOP; PRKCA; KAT14; USP36; CDK1; PHC1; METTL21A; RSBN1; PER2; TAF4; KANSL1; MYSM1; ATPSCKMT; SART3; TADA2B; NFYA; LIF; SUDS3; BRPF1; SF3B1; CHEK1; PAGR1; MSL1; KDM6A; KAT5; NCOA1; PRKAA1; UHRF1; RPS6KA5; TADA2A; SMARCAD1; SUPT7L; BARD1; SETD4; GATAD2B; DCAF1; CTNNB1; EP400; WDR82; KDM1B; TRIP12; UFL1; MLLT6; CLOCK; RRP8; MTA3; N6AMT1; NSD1; SETBP1; MAP3K7; PRKD1; SMAD4; TBL1XR1; JDP2; SUPT3H; PBXIP1; RBBP4; PCGF1; MIER1; PAXBP1; EHMT2; BRCA2; PRDM13; CHD4; ELK4; KDM4A; PHF20L1; RCOR1; MED24; MORF4L2; KAT6A; PRDM4; NELFA; ING2; PCGF3; HDAC6; EEF1AKMT3; PRKAA2; KMT5B; RBBP5; SIN3B; CDK9; CARM1; CHD3; PHF20; TWIST1; GLYR1; KAT8; AURKB; TGM2; RNF20; JADE3; EYA3; ING3; SETD2; ING5; LEO1; YEATS4; NCOA6; ATF2; CTR9; ARID4A; NSD3; MSL2; TRERF1; MEAF6; CREBBP; ABRAXAS1; TBL1X; EZH2; SUV39H2; MBIP; NAA50; PAXIP1; USP15; MCM3AP; KDM2A;
Chromosome segregation	GO:0007059	160	1.39E-18	HAUS3; CCNE2; KIF15; ZNF207; ASPM; CEP192; TPR; CDC6; KNL1; TUBGCP5; GTF2B; KNTC1; PUM2; CENPE; MKI67; FAM83D; CCSAP; CDCA2; MMS19; SMC5; CENPF; GOLGA8G; ARID2; SASS6; HASPIN; NR3C1; PDS5B; BUB1B; GOLGA8A; ARID1A; DYNC1H1; POGZ; CDT1; NCAPD3; HJURP; GOLGA2; ESCO1; FLNA; ATM; MLH3; ESPL1; CLASP2; WRAP73; CHAMP1;

				HAUS5; APC; NCOR1; NIPBL; CENPC; ERCC4; TNKS; SGO2; CLASP1; ESCO2; ATRX; NCAPH; CCNE1; PSRC1; TUBGCP3; TUBGCP4; SMARCD1; NDE1; KLHDC8B; KIF2A; ARID1B; PUM1; MAD2L1; TLK1; RIOK2; RAB11A; ANAPC5; NDC80; MIS18A; CCNB1; TTK; HAUS8; PHF13; RAD18; BRIP1; KAT5; INO80; MAD1L1; FBXO5; GEM; NEK6; EML4; SMARCAD1; MACROH2A1; SPC25; BUB1; MAP9; CENPN; NUMA1; SMARCC1; BAG6; SMC4; SPDL1; SLF2; SMC6; SKA1; EHMT2; ANAPC1; PLK1; CDC16; DLGAP5; LZTS2; GEN1; KIF18A; SPC24; FANCM; SUN1; NUP62; KIF2C; TUBB; VPS4B; HSPA1A; KNSTRN; KIFC2; CENPQ; CEP85; BIRC5; KIF22; NSL1; CDC23; TOP2A; SMC2; CEP97; SPICE1; ANAPC7; STIL; NCAPD2; MRE11; SMARCD3; CHMP4C; AURKB; ANAPC4; PBRM1; MAU2; MAP3K20; PHF10; MND1; LATS1; RMI2; AGO4; CHMP7; ACTR3; ECT2; OIP5; SMARCC2; KIF23; ABRAXAS1; MZT1; P3H4; FANCD2; NAA50; HAUS6; NCAPG; SMARCA2; HAUS2; KIF14;
Sister chromatid segregation	GO:0000819	105	3.53E-17	KIF15; ZNF207; CEP192; TPR; CDC6; GTF2B; KNTC1; CENPE; CCSAP; SMC5; CENPF; ARID2; HASPIN; PDS5B; BUB1B; ARID1A; POGZ; CDT1; NCAPD3; GOLGA2; ESCO1; FLNA; ATM; ESPL1; CLASP2; WRAP73; CHAMP1; APC; NIPBL; CENPC; TNKS; SGO2; CLASP1; ESCO2; ATRX; NCAPH; PSRC1; SMARCD1; KIF2A; ARID1B; MAD2L1; RIOK2; RAB11A; ANAPC5; NDC80; CCNB1; TTK; PHF13; KAT5; INO80; MAD1L1; FBXO5; NEK6; EML4; MACROH2A1; SPC25; BUB1; MAP9; NUMA1; SMARCC1; SMC4; SPDL1; SLF2; ANAPC1; PLK1; CDC16; DLGAP5; GEN1; KIF18A; SPC24; NUP62; KIF2C; VPS4B; HSPA1A; KNSTRN; KIFC2; BIRC5; KIF22; NSL1; CDC23; TOP2A; SMC2; CEP97; SPICE1; ANAPC7; NCAPD2; SMARCD3; CHMP4C; AURKB; ANAPC4; PBRM1; MAU2; MAP3K20; PHF10; LATS1; RMI2; CHMP7; SMARCC2; KIF23; ABRAXAS1; MZT1; NAA50; NCAPG; SMARCA2; KIF14;
Regulation of chromosome organization	GO:0033044	105	3.53E-17	HNRNPA2B1; ZNF207; TPR; CDC6; SIN3A; KNTC1; HNRNPA1; CENPE; TERF2; MCPH1; SMC5; CENPF; FEN1; ATF7IP; ARID2; HASPIN; DDX11; SETMAR; BUB1B; ARID1A; NAF1; CDT1; NCAPD3; MPHOSPH8; HMBOX1; ATM; ESPL1; AXIN2; APC; ATR; ERCC4; RESF1; YLPM1; TNKS; ATRX; NCAPH; GNL3; SMARCD1; DNMT1; ARID1B; MAD2L1; NAT10; RIOK2; ANAPC5; NDC80; SMG1; TNKS2; PIF1; CCNB1; ACTR5; TTK; MORC2; KAT5; GNL3L; INO80; MAD1L1; FBXO5; NEK6; MACROH2A1; SPC25; MAPK1; CTNNB1; BUB1; NUMA1; SMARCC1; SMC4; EID3; SPDL1; SLF2; TASOR; SMC6; HNRNPD; ANAPC1; PLK1; CDC16; DLGAP5; NSMCE4A; GEN1; SPC24; PNKP; BIRC5; CDC23; TOP2A; TENT4B; CTC1; SMC2; TRIM28; ANAPC7; MAP3K4; NCAPD2; EXOSC10; MRE11; SMARCD3; AURKB; ANAPC4; PBRM1; MAP3K20; PHF10; PRKCQ; DCP2; RMI2; SUB1; SMARCC2; NCAPG; SMARCA2;
DNA replication	GO:0006260	113	4.14E-17	CCNE2; E2F7; DNA2; BOD1L1; CDC6; NFIA; DTL; SIN3A; TBRG1; ANKRD17; KIN; ID3; TERF2; FEN1; DDX11; POLD3; GINS1; POLI; SETMAR; POLRMT; CDT1; HELB; ZRANB3; BCAR3; ESCO1; CDC7; MCM6; POLQ; E2F8; NFIC; KAT7; FAM111B; SLFN11; NOC3L; POLE2; MCM10; JADE1; ATR; GINS4; CCDC88A; RBMS1; SMARCAL1; CCNA2; WDHD1; REV1; ESCO2; ETAA1; ATRX; ORC2; CCNE1; RFC3; CDK1; LIG3; PCNA; NUCKS1; MCM4; POLA1; POLH; ACTR5; CHEK1; NFIB; GLI2; INO80; FBXO5; RAD17; ZNF830; BARD1; POLK; RBBP6; RFWD3; LPIN1; RBBP4; CINP; EHMT2; EGFR; BRCA2; CHAF1A; MCM5; GEN1; MCM8; MCM9; EXD2; FANCM; WRN; TICRR; GINS3; ZPR1; DBF4B; RPA2; LIG1; RFC1; PNKP; RNASEH1; CTC1; SENP2; CDK9; CARM1; ZBTB38; ORC4; MRE11; JADE3; RMI2; ING5; TIPIN; POLG; ORC1; REV3L; MEAF6; MCMBP; ZNF365; BAZ1A; PRIM2; NASP;

H9N2 Upregulated DEGs Pathway Analysis

H9N2 Upregulated

KEGG Pathway	Count	P-Value	Genes

Influenza A	30	3.5E-21	OAS1; OAS2; OAS3; CCL5; CXCL10; JAK2; MX1; MX2; MYD88; PML; RIGI; TNFSF10; CASP1; CASP8; EIF2AK2; IFNB1; IFIH1; IRF7; IRF9; IL12A; IL6; PIK3R3; RSAD2; RNASEL; STAT1; STAT2; SOCS3; TLR3; TRIM25; TNF;
Hepatitis C	22	2.5E-13	OAS1; OAS2; OAS3; CXCL10; MX1; MX2; RIGI; CASP8; CLDN23; EIF2AK2; IFNB1; IFIT1; IRF7; IRF9; PIK3R3; RSAD2; RNASEL; STAT1; STAT2; SOCS3; TLR3; TNF;
NOD-like receptor signaling pathway	23	7.3E-13	OAS1; OAS2; OAS3; CCL5; MYD88; TNFAIP3; BIRC3; CASP1; CASP8; CARD16; GBP1; GBP2; GBP3; GBP4; IFNB1; IFI16; IRF7; IRF9; IL6; RNASEL; STAT1; STAT2; TNF;
Measles	20	2.0E-12	OAS1; OAS2; OAS3; MX1; MX2; MYD88; RIGI; TNFAIP3; CASP8; EIF2AK2; Hsp70; HSPA1A; IFNB1; IFIH1; IRF7; IRF9; IL12A; IL6; PIK3R3; STAT1; STAT2;
Epstein-Barr virus infection	22	3.1E-11	OAS1; OAS2; OAS3; BLNK; CXCL10; ISG15; MYD88; RIGI; TNFAIP3; CASP8; EIF2AK2; IFNB1; IRF7; IRF9; IL6; HLA-E; PIK3R3; STAT1; STAT2; TAP1; TAP2; TNF;

H9N2 Upregulated

GO Enrichment Analysis	GO ID	Count	P-Value	Genes
Response to virus	GO:0009615	82	6.61E-70	RSAD2; IFIT3; IFIH1; IFIT2; IFIT1; IFNL2; IFI27; IFI44L; RIGI; CCL5; HERC5; IFNL1; IFITM1; OASL; NLRC5; IFI16; ISG20; IRF1; TRIM21; MX1; TLR3; OAS1; SAMHD1; PARP9; DDX60L; DDX60; IRF7; STAT2; IFNB1; IFI44; DTX3L; GBP1; STAT1; IFI6; MLKL; OAS2; SHFL; MX2; ZNFX1; PLSCR1; IRF9; IFIT5; ISG15; TRIM25; IFNL3; CXCL10; NT5C3A; TRIM31; CASP1; IRF2; PMAIP1; TRIM38; ZC3HAV1; GBP3; MYD88; NMI; PML; EIF2AK2; TRIM22; TRIM26; JAK2; IFITM3; ITGB6; TRIM56; AZI2; LGALS9; TRIM5; IL6; TRIM34; RTP4; TNFAIP3; IFITM2; IL15; GATA3; BST2; TNF; OAS3; RNASEL; BCL3; IL12A; ZBP1; LYST;
Defense response to virus	GO:0051607	72	1.30E-66	RSAD2; IFIT3; IFIH1; IFIT2; IFIT1; IFNL2; IFI27; IFI44L; RIGI; HERC5; IFNL1; IFITM1; OASL; NLRC5; IFI16; ISG20; IRF1; TRIM21; MX1; TLR3; OAS1; SAMHD1; PARP9; DDX60L; DDX60; IRF7; STAT2; IFNB1; DTX3L; GBP1; STAT1; IFI6; MLKL; OAS2; SHFL; MX2; ZNFX1; PLSCR1; IRF9; IFIT5; ISG15; TRIM25; IFNL3; CXCL10; NT5C3A; TRIM31; CASP1; IRF2; PMAIP1; TRIM38; ZC3HAV1; GBP3; MYD88; PML; EIF2AK2; TRIM22; TRIM26; IFITM3; TRIM56; AZI2; TRIM5; IL6; TRIM34; RTP4; TNFAIP3; IFITM2; IL15; BST2; OAS3; RNASEL; ZBP1; LYST;
Defense response to symbiont	GO:0140546	72	1.68E-66	RSAD2; IFIT3; IFIH1; IFIT2; IFIT1; IFNL2; IFI27; IFI44L; RIGI; HERC5; IFNL1; IFITM1; OASL; NLRC5; IFI16; ISG20; IRF1; TRIM21; MX1; TLR3; OAS1; SAMHD1; PARP9; DDX60L; DDX60; IRF7; STAT2; IFNB1; DTX3L; GBP1; STAT1; IFI6; MLKL; OAS2; SHFL; MX2; ZNFX1; PLSCR1; IRF9; IFIT5; ISG15; TRIM25; IFNL3; CXCL10; NT5C3A; TRIM31; CASP1; IRF2; PMAIP1; TRIM38; ZC3HAV1; GBP3; MYD88; PML; EIF2AK2; TRIM22; TRIM26; IFITM3; TRIM56; AZI2; TRIM5; IL6; TRIM34; RTP4; TNFAIP3; IFITM2; IL15; BST2; OAS3; RNASEL; ZBP1; LYST;
Negative regulation of viral process	GO:0048525	37	3.48E-44	RSAD2; IFIH1; IFIT1; CCL5; IFITM1; OASL; IFI16; ISG20; TRIM21; MX1; OAS1; IFNB1; STAT1; OAS2; SHFL; TRIM14; ZNFX1; PLSCR1; IFIT5; ISG15; TRIM25; IFNL3; TRIM31; ZC3HAV1; EIF2AK2; TRIM26; IFITM3; TRIM5; FAM111A; CH25H; IFITM2; N4BP1; PTX3; BST2; TNF; OAS3; RNASEL;
Regulation of viral process	GO:0050792	42	6.61E-40	RSAD2; IFIH1; IFIT1; CCL5; IFITM1; OASL; IFI16; LAMP3; ISG20; TRIM21; MX1; OAS1; IFNB1; STAT1; OAS2; SHFL; TRIM14; ZNFX1; PLSCR1; IFIT5; ISG15; TRIM25; IFNL3; TRIM31; TRIM38; ZC3HAV1; EIF2AK2; TRIM22; TRIM26; IFITM3; LGALS9; TRIM5; FAM111A; TRIM34; CH25H; IFITM2; N4BP1; PTX3; BST2; TNF; OAS3; RNASEL;

H9N2 Downregulated DEGs Pathway Analysis

H9N2 Downregulated

KEGG Pathway	Count	P-Value	Genes
TGF-beta signaling pathway	5	3.7E-03	GREM1; ID2; THBS1; TFRC; TGFB2;
Regulation of actin cytoskeleton	5	4.5E-02	IQGAP1; ITGB4; MYH10; MYH9; RGCC;

H9N2 Downregulated

GO Enrichment Analysis	GO ID	Count	P-Value	Genes
Rhythmic process	GO:0048511	10	9.83E-06	DBP; HLF; CBX3; SREBF1; DHX9; TGFB2; HNRNPD; KLF9; ID2; EGR1;
Response to decreased oxygen levels	GO:0036293	10	1.07E-05	CCN2; TFRC; MALAT1; RGCC; HILPDA; HP1BP3; SLC11A2; TGFB2; THBS1; EGR1;
Fibroblast migration	GO:0010761	5	1.58E-05	IQGAP1; AKAP12; PLEC; THBS1; ZFAND5;
Response to oxygen levels	GO:0070482	10	2.22E-05	CCN2; TFRC; MALAT1; RGCC; HILPDA; HP1BP3; SLC11A2; TGFB2; THBS1; EGR1;
Ameboidal-type cell migration	GO:0001667	12	2.80E-05	GREM1; RGCC; MYH9; SOX17; NANOS1; IQGAP1; TGFB2; ITGB4; AKAP12; PLEC; THBS1; ZFAND5;